



Development of double emulsion nanoparticles for the encapsulation of bovine serum albumin



Nelida.Y. Martinez^{a,*}, Patricia F. Andrade^b, Nelson Durán^{b,c,d}, Sebastian Cavalitto^a

^a Centro de Investigación en Fermentaciones Industriales CINDEFI, UNLP-CONICET-CCT La Plata, Facultad de Cs Exactas, Universidad Nacional de La Plata, Calle 50 # 227, 1900 La Plata Argentina

^b University of Campinas (UNICAMP), Institute of Chemistry (IQ), Biological Chemistry Laboratory, CP 6152, CEP 13083-970, Campinas, SP, Brazil

^c Brazilian National Nanotechnology Laboratory (LNNano-CNPEM), Campinas, Brazil

^d NanoBioss (MCTI), IQ-UNICAMP, Campinas, Brazil

ARTICLE INFO

Article history:

Received 25 March 2017

Received in revised form 7 June 2017

Accepted 21 June 2017

Available online 29 June 2017

Keywords:

Double emulsion nanoparticles

Bovine serum albumin encapsulation

Poly-ε-caprolactone

Pluronic F68

Hydrophobic interactions

ABSTRACT

In the present work, a double emulsion was developed for the encapsulation of Bovine Serum Albumin (BSA) as a model protein for the future encapsulation of viral proteins. The first emulsion polydispersity index (PDI) was studied with increasing concentrations of poly (ε-caprolactone) (PCL) as stabilizer (from 16% w/v to 5% w/v) and polyvinyl alcohol (PVA) as the surfactant in the second emulsion at 1.5% w/v. Results suggest that at decreasing concentrations of PCL the PDI of the emulsion also decrease, indicating that viscosity of the emulsion is crucial in the homogeneity of the resultant size distribution of the nanoparticles. When PVA concentration in the second emulsion was increased from 1.5% w/v to 2.5% w/v the PDI also increased. To study the relationship between the structure of the surfactant in the second emulsion and the resultant BSA encapsulation, emulsions were prepared with Pluronic F68 and PVA both at 1.5% w/v and PCL in the first emulsion at 5% w/v. Results indicated that Pluronic F68 was a better stabilizer because at the same experimental conditions encapsulation of BSA was 1.5 higher than PVA. FTIR studies confirmed the presence of BSA in the nanoparticles. SEM and TEM microscopies showed a size distribution of 300 nm–500 nm size of nanoparticles. Circular dichroism studies demonstrated that the secondary structure of the protein was conserved after the encapsulation into the nanoparticles.

© 2017 Elsevier B.V. All rights reserved.

1. Introduction

The encapsulation of proteins into polymeric nanoparticles is a promising methodology to provide protection against hostile environmental conditions for proteins (e.g., pH, T, proteolysis) [1]. Even more, encapsulation of proteins into nanoparticles prepared by double emulsion methodology is a fine alternative widely used nowadays because of high loading efficiency, controlled release kinetics and preservation of secondary structure of proteins [2]. This item is crucial for adjuvancy, vaccination and enzymatic treatment of pathologies [3]. Nanoparticles developed by double emulsion used for adjuvancy have the advantage of controlled size distribution from 60 to 600 nm. Size is important for immune response where dendritic cells prefer to uptake particles with less than 500 nm. Macrophages, however, preferentially uptake particles with size ranging from 0.5 to 5 μm [4].

So far, several proteins have been encapsulated into polymeric nanoparticles via double emulsion synthesis with promising results such as high encapsulation efficiency ($\geq 70\%$), homogeneous distribution of the protein into nanoparticles and controlled release [5]. For vaccination purposes, diphtheria toxoid (DT) antigen has been encapsulated into polymeric poly(ε-caprolactone) (PCL) double emulsion nanoparticles with secondary structure preservation. This allowed significant DT specific immune response in comparison with free DT antigen [6].

Double emulsion synthesis of nanoparticles is a fast and cost effective procedure. The first emulsion is developed by mixing the aqueous phase of proteins or hydrophilic drugs into an oil phase composed of a surfactant dissolved in a solvent. In this first step, the aqueous droplets are stabilized by the surfactant immersed in the oil phase. This first emulsion is mixed into an aqueous phase composed of another surfactant of choice where the oil droplets are stabilized by a second surfactant. Among the most used surfactants for the development of the first emulsion are PCL, polyethylene glycol (PEG) and poly(lactic-co-glycolic acid) (PLGA). For the second emulsion, polymers like polyvinyl alcohol and Pluronic have been

* Corresponding author.

E-mail address: yanmartar@gmail.com (Nelida.Y. Martinez).

used with fine results [7–9], because of homogenous size distributions and less coalescence of particles where reported.

The polymeric material used for the development of such nanoparticles for health applications must be biodegradable, biocompatible and non-toxic. In this scenario, PCL is Generally Recognized as Safe (GRAS) (FDA) widely used for biomedical applications such as tissue engineering, development of scaffolds for cell adherence and regeneration of bone [10]. Unlike most polymers, PCL is cheaper. In this regard, this is very important when scaling up. Also, it has been reported that super hydrophobic materials slow down release of hydrophilic molecules. In this sense, it has been reported that an anticancer drug was released for 15 days from microfibers of PCL [11]. Poly vinyl alcohol (PVA) is another polymer widely used for first emulsions stabilization and protein encapsulation since good results were obtained for encapsulation of proteins (encapsulation efficiency of 50%). PVA is a FDA approved polymer used in commercial products like eye lenses [12], scaffold development for cell attachment and drug delivery [13,14].

In order to obtain homogenous particle size emulsions, some parameters have to be set up like surfactants molecular weight and concentration, solvent evaporation and initial concentration of protein or drugs. Sonication is widely used for emulsion development since is a fast and reproducible methodology.

In the present work, double emulsion nanoparticles were developed for the encapsulation of Bovine Serum Albumin (BSA) as a model protein. PCL was the surfactant of choice for the first emulsion because of the characteristics mentioned before. PVA and Pluronic F68 were used for second emulsion stabilization in order to study the effect of concentration of surfactant on BSA encapsulation percent. In the present article, the word *nanoparticle* refers to the outer water in oil droplet, meaning the nanoparticles composed of both emulsions where the first emulsion is used to stabilize the inner aqueous droplets immersed in the solvent and the second emulsion is used to stabilize the whole system immersed in the outer aqueous solution.

The formulations were characterized by electronic microscopy, transmission electron microscopy and dynamic light scattering. The presence of BSA into the nanoparticles was studied by FTIR spectroscopy. In future experiments, a viral protein will be encapsulated in the characterized formulations of the present work for vaccination purposes.

2. Materials and methods

2.1. Materials

Bovine serum albumin (BSA) (fraction V) from Sigma Aldrich, Poly (ϵ - caprolactone) (PCL) of MW 70–90 kDa, PVA of MW 72 kDa hydrolysis degree of 99%, Pluronic F68 MW 8350 Da from Sigma Aldrich and lipid were kindly provided by Biologic Chemistry Lab, Institute of Chemistry, UNICAMP, Brazil. Chloroform reagent was acquired from J.T Baker.

2.2. Synthesis of nanoparticles

100 mg of lipid were dissolved in 1 ml of chloroform and then 5% w/v, 10% w/v and 16% w/v of PCL were added, dissolved and mixed vigorously in order to provide a good interaction of the oil phase with the surfactant. Then 5 mg of BSA were dissolved in 200 μ l of distilled water. This was considered the aqueous phase. The aqueous phase was mixed with the oil phase by sonication during 1 min in an ice bath in order to obtain the first emulsion. As explained before, in this first emulsion the aqueous droplets formed by sonication are stabilized into the oil phase by the presence of surfactant PCL, where the hydrophilic groups of PCL interact with the aqueous

phase and the hydrophobic tail of PCL interacts with the oil phase. Control experiments were performed with 200 μ l of distilled water.

The resultant first emulsion was mixed by sonication during 2 min in an ice bath with 6 ml of 1.5% w/v, 2.0% w/v and 2.5% w/v of PVA or 6 ml of 1.5 w/v, 1.0% w/v, 0.5% and 0.1% w/v of Pluronic F68 dissolved in distilled water. The resultant double emulsion was solvent evaporated by rotation or stirring for 3 h and centrifuged for 10 min at $10.000 \times g$ in order to separate microparticles from nanoparticles. After centrifugation, the supernatant was recovered and centrifuged for 20 min at $12.000 \times g$. The pellet was suspended in the same volume and the nanoparticles were stored at 5 °C for further experiments.

2.3. Loading of BSA into nanoparticles

Loading of BSA was calculated after measuring BSA concentration before and after the nanoparticles preparation. In this direction, nanoparticles were centrifuged for 20 min at $12.000 \times g$ and supernatant protein was measured with Bradford Reagent at 595 nm. The difference between the initial and supernatant concentration per mg of nanoparticles was considered as the mg of protein encapsulated into mg of nanoparticles. Control determinations were done with nanoparticles with no BSA.

2.4. Characterization of nanoparticles

2.4.1. Dynamic light scattering (DLS) of nanoparticles

The nanoparticles were characterized by Dynamic Light Scattering (DLS) and size distribution was observed by polydispersity index (PDI) values. Measurements were analyzed in a ZetaSizer nano Zen 3600 Malvern. Except for Table 3 samples which were analyzed in a Malvern Instrument Model Nano Z 590.

2.4.2. Electronic microscopy of nanoparticles

The morphology and size of nanoparticles was studied using an electronic microscopy with field emission source, model FEI Quanta FEG250, using 5 kV and 10 kV. A droplet of nanoparticles was deposited at a stub of silica fixed with carbon tape and dried at ambient temperature of 25 °C, then covered with a fine layer of carbon and gold using a metallizer Baltec MED 020.

2.4.3. Transmission electron microscopy of nanoparticles

Nanoparticles size and shape were analyzed with a Tecnai F20 (G^2) operated at 200 kV and room temperature.

2.4.4. FTIR-ATR study of BSA and NP loaded BSA

Dried samples were studied in a Perkin Elmer model Spectrum Two and samples were measured with a UATR (Single Reflection Diamond) accessory.

2.4.5. Circular dichroism of BSA and NP loaded BSA

The circular dichroism measurements of free BSA and encapsulated BSA into NP were performed in a Jasco 720 Spectropolarimeter at room temperature (23 °C) using quartz cuvettes with 10 mm path length. The average of 8 scans per sample was collected as one spectrum.

3. Results and discussion

3.1. Nanoparticles formulation, relationship between surfactant concentration and size distribution of resultant nanoparticles

3.1.1. Effect of PCL concentration on PDI

Experiments were done with PCL concentration from 5% w/v to 16% w/v in the first emulsion and PDI index values of the resultant nanoparticles were observed as well as size distribution. The

Table 1

PCL concentration relationship with size distribution of resultant nanoparticles (PVA concentration was fixed at 1.5% w/v).

PCL(% w/v)	PDI	Size(nm)
16	0.89 ± 0.016	1398
10	0.45 ± 0.015	320.2
5	0.37 ± 0.011	331.2

(SD, n = 2)

Table 2

PVA concentration effect on polydispersity index. PCL concentration was fixed at 5% w/v.

PVA (% w/v)	PDI	Size (nm)
1.5	0.370 ± 0.1	331.2
2.0	0.614 ± 0.1	1269.0
2.5	0.622 ± 0.1	1307.0

(SD, n = 2)

Table 3

Effect of Pluronic F68 concentration on PDI. PCL concentration was fixed at 5.0% w/v.

Pluronic F68 (% w/v)	PDI	Size (nm)
1.5	0.25 ± 0.03	331.2
1.0	0.28 ± 0.02	322.9
0.5	0.41 ± 0.04	840.0

(SD, n = 2)

polydispersity index is the degree of non-uniformity of the distribution size of a formulation where a monodisperse distribution has a PDI = 0.0 and a moderate polydispersity distribution type has a PDI value ranging from 0.1 to 0.4.

In all cases PVA concentration was fixed at 1.5% w/v. **Table 1** results show a decrease in PDI values as PCL concentration decrease, in other words there might be a relationship between PCL concentration and the resultant homogeneity of the size distribution of the nanoparticles. This effect has been reported by other authors when an increase in first emulsion polymer concentration shows an increase in polydispersity of nanoparticles size because an increase in viscosity in the first emulsion generates an instable dispersion of water droplets into the oil phase. In this sense, first emulsion instability reduces the efficiency of formation of droplets in the second emulsion [8]. When 5.0% w/v PCL concentration was used, PDI values were 0.370 ± 0.011 . Future experiments were conducted using this PCL concentration because these PDI values agree with a homogenous size distribution. The type of distribution size is monomodal.

It is important to cite that the size of the inner aqueous droplets was not measured in the present work. The assumption that an increase in PCL concentration will change the resulting outer emulsion is based on viscosity increase by increasing PCL concentration. In this sense, instable inner aqueous droplets are formed and in consequence they coalesce forming bigger droplets. This is confirmed by the increasing size of the resulting nanoparticles as the PCL concentration is increased.

3.1.2. Effect of PVA concentration on PDI

When PCL concentration was fixed at 5.0% w/v and PVA concentration was adjusted to 2.0% w/v and 2.5% w/v, a heterogeneous size distribution was observed indicating that higher concentrations of PVA leads to higher polydispersity in the final formulations as well as higher nanoparticles size. Results are shown in **Table 2**. It is possible that at higher polymer concentration, the viscosity of the second emulsion increase and in consequence breaking the emulsion into smaller droplets is less probable. That is to say that breaking the emulsion into smaller droplets is no longer possible because the

sintering energy achieved by the increasing power output required for higher viscosity of the solution, generates sintering and coalescence of the nanoparticles. It is true that the higher the viscosity of the solution, the higher the power output and in consequence more breaking droplets take place. However, there is an inflection point where the sintering energy achieved generates coalescence between particles forming larger particles.

Also, it is possible that residual PVA in the solution forms aggregates.

3.1.3. Effect of solvent evaporation methodology on PDI

As described before, solvent evaporation was done by rotary evaporation at ambient temperature (26 °C). Solvent evaporation is a crucial step in the formation of nanoparticles. If the solvent is not well evaporated, the resulting size particle is not homogenous because of solvent residues present in a population of nanoparticles with higher size [5].

Hence, nanoparticles were prepared with PCL 5.0% w/v, PVA 1.5% w/v and solvent evaporation was done by stirring for 3 h at 26 °C to study the evaporation method effect on PDI values. Resulting PDI values were 0.233 ± 0.01 and size was 247.5 nm. Comparing rotary with stirring solvent evaporation methodology, the latter shows a more homogeneous size distribution and smaller particle size. Besides, for experimental purposes is more useful because several formulations can be synthesized at the same time. In this way, further experiments were done with solvent evaporation by stirring.

3.1.4. Effect of pluronic F68 concentration on PDI

PCL concentration was fixed at 5.0% w/v and Pluronic F68 concentration was varied from 0.5% w/v to 1.5% w/v. This concentration range was chosen because as mentioned before, at concentrations higher than 1.5% w/v of polymer, the viscosity of solution increased leading to higher nanoparticles size. In the present work, the viscosity of 1.5% w/v of PVA or Pluronic F68 solution was not measured. Nevertheless, according to the results shown in **Table 2** it was assumed that the higher concentrations of PVA (>1.5% w/v) led to increased viscosity of the solution because higher size of nanoparticles were observed. This effect was also observed by Stoppel et al., when increasing the concentration of Pluronic F68 from 0.0 to 2.0% w/v the beads size increased from 7 µm to 11 µm where beads were developed with alginate and Pluronic F68 by ionic gelation. This effect was attributed to higher viscosity of the solutions when increasing concentrations of Pluronic F68 [15].

All formulations were synthesized by rotary evaporation of solvent. Results are shown in **Table 3**. As Pluronic F68 concentration decrease, PDI increase showing a relationship between size distribution and surfactant concentration. As Pluronic F68 concentration decrease, the stability of the emulsion is badly affected leading to nanoparticles with a heterogeneous size distribution.

3.2. BSA encapsulation. effect of type of surfactant on encapsulation of BSA

In order to study BSA encapsulation loading with the type of polymer present in the second emulsion, nanoparticles were prepared with 5.0% (w/v) of PCL w/v and 1.5% w/v PVA or Pluronic F68. Results show that using Pluronic F68 as emulsifier in the second emulsion, a higher BSA encapsulation percent was achieved of $76.0 \pm 1.7\%$ compared to $49.1 \pm 7.6\%$ using PVA.

In presence of Pluronic F68, a higher encapsulation percentage was achieved probably because a more hydrophilic environment favours BSA retention into the aqueous droplets immersed in the oil phase. This was previously reported by [16]. Because of Pluronic F68 amphiphilic structure, the hydrophobic PPO (polypropylene oxide) chains interact with the hydrophobic environment while

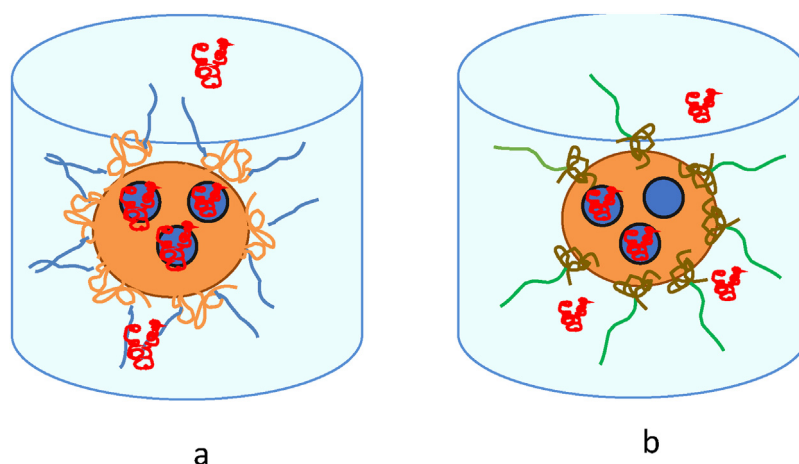


Fig. 1. 1a. Schematic representation of Pluronic F68 stabilizing the first emulsion immersed in the oil phase where PPO chains are orange coloured and PEO chains are blue coloured. 1b PVA as stabilizing agent where —OH groups are in green and carbon hydrophobic chain is shown in brown. (For interpretation of the references to colour in this figure legend, the reader is referred to the web version of this article.)

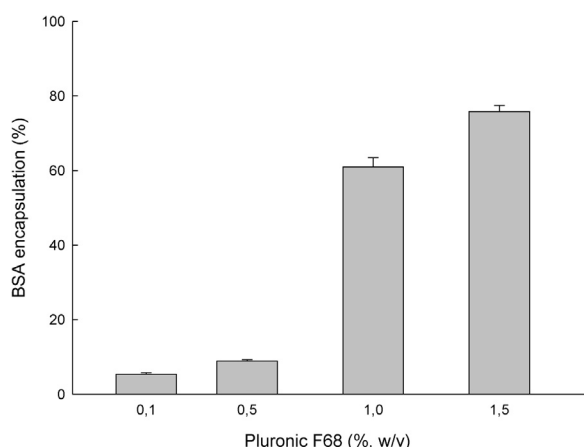


Fig. 2. Relationship between BSA encapsulation (%) and Pluronic F68 concentration (w/v).

the hydrophilic PEO (polyethylene oxide) chains interact with the aqueous external phase. PVA, however, have a different chemical structure of side chains than Pluronic F68. In this way, Pluronic F68 is a better stabilizer of the emulsion because at the same experimental conditions has more hydrophilic residues to interact with water and in consequence BSA encapsulation is favoured because a more stable emulsion is achieved using this surfactant in the second emulsion (see Fig. 1). In this way, BSA diffuses to the outer aqueous phase because of instability of the second emulsion shell which is unable to retain BSA molecules.

In order to establish a relationship between Pluronic F68 concentration and BSA encapsulation percent, Pluronic F68 concentration used was 1.5, 1.0, 0.5 and 0.1% w/v. Results are shown in Fig. 2. An increase in Pluronic F68 concentration related with an increase in BSA encapsulation can be explained in one hand, because of Pluronic F68 chemical structure which allows second emulsion stabilization. On the other hand, there might be an interaction between BSA and the polymer. As shown in Fig. 2, BSA encapsulation of $76.0 \pm 1.7\%$ is achieved at 1.5% w/v of Pluronic F68.

It was possible to observe that there is a “jump” in the encapsulation of BSA (%) between 0.5% w/v and 1.0% w/v of Pluronic F68. This could be explained by the relationship between the critical micellar concentration of Pluronic and the stability of the emulsion. In a previous work where w/o emulsion were prepared using Pluronic F68 as surfactant, it was reported that beyond 7.8×10^{-4} mol/L

of Pluronic F68, the emulsion destabilized quickly and nanoparticles coalesce. Between 7.8×10^{-4} mol/L and 3.1×10^{-3} mol/L of Pluronic F68 emulsions were stable [17]. In the present work at 6.0×10^{-4} mol/L of Pluronic F68 (0.5% w/v) the encapsulation of BSA was low, probably because an instable emulsion is formed at this experimental conditions so the BSA was released to the outer aqueous phase. When the concentration of Pluronic F68 was increased to 1.0% (w/v) (1.0×10^{-3} mol/L) the encapsulation of BSA was widely increased because at this concentration of Pluronic F68 the stability of the emulsion also increased. In this way, DLS measurements on Table 3 are in agreement with these conclusions where at decreasing concentrations of Pluronic F68, PDI values increased perhaps because of the instability of the emulsion and the coalescence of the nanoparticles. Hence, BSA diffuses to the outer aqueous phase because of instability of the shell made by the second emulsion which is unable to retain BSA molecules.

3.3. FTIR studies of samples

FTIR studies were used to observe a possible interaction between BSA and the nanoparticles. Fig. 3a shows IR spectra from 4000 cm^{-1} and 500 cm^{-1} of pure BSA, encapsulated BSA and control nanoparticles. According to literature [18], BSA amide I band related to C=O stretching is in the region of $1600\text{--}1700\text{ cm}^{-1}$ and amide II band related to C—N stretching is in the region of 1540 cm^{-1} . Amide I and II bands of pure BSA are indicated in the spectra with arrows at 1643 cm^{-1} and 1532 cm^{-1} respectively. As can be observed, control nanoparticles have no signal at BSA amide II band which is expected because amide is not present in PCL or Pluronic F68 chemical structure. There is a signal, however, at 1652 cm^{-1} attributed to carbonyl compound of PCL. Encapsulated BSA spectra show a signal peak at 1652 cm^{-1} for amide I and 1549 cm^{-1} for amide II region indicating the presence of BSA into the nanoparticles. This hypsochromic shift to higher energy from 1643 cm^{-1} to 1652 cm^{-1} for amide I and 1532 cm^{-1} to 1549 cm^{-1} for amide II in the absorption spectra shows that a hydrophobic interaction between BSA and the matrix is probable. Fig. 3b shows a zoomed spectra in the region due to antisymmetric angle bending of CH_3 at 1450 cm^{-1} and angle bending of CH_2 group at 1391 cm^{-1} groups for pure BSA. Encapsulated BSA shows a signal at 1472 cm^{-1} corresponding to CH_3 groups and 1396 cm^{-1} for CH_2 group signal. This hypsochromic shift to higher energy for CH_3 and CH_2 groups may indicate a hydrophobic interaction of BSA with the hydrophobic tails of surfactants.

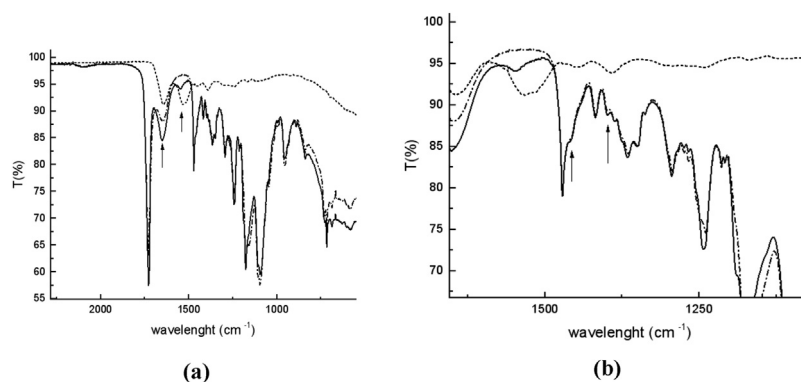


Fig. 3. a FTIR spectra of pure BSA (short dash), encapsulated BSA into NP (straight line) and control NP without BSA (dash dot). Arrows show Amide I and Amide II bands. b Zoomed region from 1654 cm^{-1} to 1069 cm^{-1} . Arrows show CH_3 and CH_2 bands.

These results suggest that BSA is incorporated in the nanoparticles forming hydrophobic interactions between BSA and carbonyl tails of surfactants and lipid. After the double emulsion is developed, the protein locates at the interface between the aqueous phase and the oil phase. This conclusion was also observed when BSA was encapsulated into solid lipid nanoparticles [19].

In a previous work, BSA was exposed to heat condition in presence of tween 20 and no secondary structure change was observed. These results indicate that tween surfactant binds to hydrophobic pockets of BSA [20]. In another work, PPO residues were exposed to BSA increasing concentrations from 0 to 0.5 mg/ml and micellization was monitored. At increasing concentrations of BSA, micelle formation was impeded by hydrophobic interactions of BSA with PPO [21]. Besides, when BSA and amphiphiles like 2-alkylmalonic acid and 2-alkylbenzimidazole interactions were studied, a hypsochromic blue shift of the BSA fluorescence spectra was found at increasing concentrations of 2-alkylmalonic acid but not in presence of 2-alkylbenzimidazole. It was suggested that the length of the carbon chain is crucial for hydrophobic interactions [22].

FTIR results in the present work are in agreement with encapsulation results where an increasing concentration of Pluronic F68 leads to an increase in BSA encapsulation. In this sense, a model is proposed where BSA is located at the interface between the oil phase and the aqueous phase. As Pluronic F68 concentration increase, a more stable emulsion is achieved and a higher amount of BSA is able to interact with the matrix. A schematic representation is shown in Fig. 4a.

3.4. Circular dichroism of free and encapsulated BSA

The secondary structure of proteins can be monitored through circular dichroism spectroscopy. In the present work, this methodology was used to study if the secondary structure of the protein is affected by the encapsulation process into the nanoparticles. It is known that exposure to solvent and temperature can affect the structure of a protein. Probably the use of solvent in the synthesis might be a parameter that affect the secondary structure of the protein. Fig. 4b shows the circular dichroism spectrum of free BSA and encapsulated BSA into the nanoparticles. The α -helix domains in the spectrum are the valleys at 209 and 222 nm. The peak at 215 nm correspond to β -sheets domains. It is observed that the secondary structure of encapsulated BSA is slightly affected compared to free BSA. A cause of this might be explained by the results obtained previously by FTIR spectroscopy where hydrophobic interactions were proposed between BSA and the matrix. These conclusion was also reported in another work where BSA was encapsulated in PLA nanoparticles and the secondary structure of the protein was slightly affected. In that case, hydrophobic interactions between the protein and the nanoparticles were observed [23]. Besides when BSA was absorbed in polystyrene nanoparticles, changes in the secondary structure were observed according to a previous work [24].

3.5. Morphology of nanoparticles

Fig. 5a shows the morphology of BSA nanoparticles studied by scanning electron microscopy (SEM) with dimensions according to

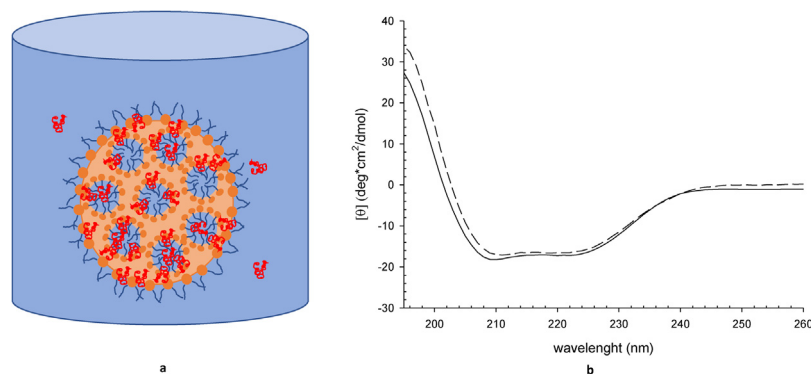


Fig. 4. a Schematic representation w/o/w emulsion where BSA (red) is located at the interface through hydrophobic interaction between the oil phase (orange) and the aqueous phase (blue). PCL is located around the inner aqueous droplets and Pluronic F68 is localized in the outer aqueous phase stabilizing the whole system. b Circular dichroism spectra of free BSA (solid line) and encapsulated BSA into the nanoparticles (dash line). (For interpretation of the references to colour in this figure legend, the reader is referred to the web version of this article.)

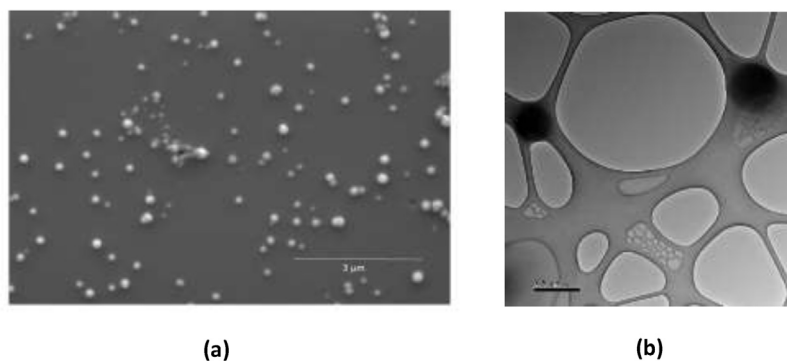


Fig. 5. (a) SEM images of BSA nanoparticles composed of PCL 5.0% w/v, Pluronic F68 1.5% w/v. (b) TEM image of nanoparticles with 500 nm and 300 nm size.

light scattering studies around 300 nm. Fig. 5b shows a TEM image of BSA nanoparticles size corresponding to 300 nm and 500 nm. These results are also in agreement with DLS and SEM microscopy.

4. Conclusion

In the present work, nanoparticles of 300–500 nm were prepared using a double emulsion methodology. Size distribution and polydispersity index (PDI) were used to monitor nanoparticles synthesis. A relationship between PCL concentration and PDI was observed. As PCL concentration decreased, a more homogenous size dispersion was achieved. As reported before, viscosity of emulsions plays an important role in resultant size distribution of nanoparticles. Also when PVA concentration was increased from 1.5% w/v to 2.5% w/v, size distribution was badly affected. Then, the concentration of the emulsifier in the first and in the second emulsion must be checked in order to obtain fine results.

The effect of Pluronic F68 concentration on the encapsulation of BSA showed an increase in BSA encapsulation as Pluronic F68 concentration increased. This results were explained by FTIR studies where BSA binds to the polymeric emulsion by hydrophobic interactions, in this way it is expected that both the hydrophobic interactions plus the chemical structure of Pluronic F68 side chains leads to an increase in BSA encapsulation while Pluronic F68 concentration increases stabilizing the double emulsion.

Size of nanoparticles studied by TEM and SEM microscopy agreed with DLS results. Besides the secondary structure of the protein was slightly affected after encapsulation protocol, this might be explained in terms of the hydrophobic interactions between the BSA and the matrix. In summary, the use of w/o/w emulsion for the encapsulation of proteins is a promising methodology for the encapsulation of viral proteins in future works because a high encapsulation percent is achieved and secondary structure is conserved.

Acknowledgements

The authors would like to thank to the Institute of Chemistry, Biological Chemistry Laboratory, Universidade Estadual de Campinas, UNICAMP, Campinas, SP, Brazil for the facilities provided and also to FAPESP, INOMAT (MCTI/CNPq) and NanoBioss (MCTI) from Brazil.

Thanks to Dr. Vázquez Mansilla Marcelo y Dr. Enio Junior from the Comisión Nacional de Energía Atómica. Gerencia del área de Investigación y Aplicaciones No Nucleares. Gerencia de Física (Centro Atómico Bariloche) Argentina for the use of FTIR-ATR spectrometer and DLS in Table 3. Also to Dr Sergio Moreno from the Material Area of CNEA, CONICET, Centro Atómico Bariloche, S. C. de Bariloche, Río Negro, Argentina for TEM images studies.

References

- [1] J. Wu, N. Kamaly, J. Shi, L. Zhao, Z. Xiao, G. Hollett, R. John, S. Ray, Development of multinuclear polymeric nanoparticles as robust protein nanocarriers, *Angew. Chem. Int. Ed. Engl.* 53 (2014) 8975–8979.
- [2] J.-H. Kim, A. Taluja, K. Knutson, Y.H. Han Bae, Stability of bovine serum albumin complexed with PEG-poly(L-histidine) diblock copolymer in PLGA microspheres, *J. Control. Rel.* 109 (2005) 86–100.
- [3] V.E. Bosio, G.A. Islan, Y.N. Martinez, N. Durán, G.R. Castro, Nanodevices for the immobilization of therapeutic enzymes, *Crit. Rev. Biotechnol.* 36 (2016) 447–464.
- [4] S.D. Xiang, A. Scholzen, G. Minigo, C. David, V. Apostolopoulos, P.L. Mottram, M. Plebanski, Pathogen recognition and development of particulate vaccines: does size matter? *Methods* 40 (2006) 1–9.
- [5] Y.-Y. Yang, T.-S. Chung, N.P. Ngee, Morphology, drug distribution, and in vitro release profiles of biodegradable polymeric microspheres containing protein fabricated by double-emulsion solvent extraction/evaporation method, *Biomaterials* 22 (2001) 231–241.
- [6] J. Singh, S. Pandit, V.W. Bramwell, H.O. Alpar, Diphtheria toxoid loaded poly(ϵ -caprolactone) nanoparticles as mucosal vaccine delivery systems, *Methods* 38 (2006) 96–105.
- [7] N. Teekamp, L.F. Duque, H.W. Frijlink, W.L.J. Hinrichs, P. Olinga, Production methods and stabilization strategies for polymer-based nanoparticles and microparticles for parenteral delivery of peptides and proteins, *J. Polym. Res.* 12 (2015) 1311–1331.
- [8] C. Giovino, I. Ayensu, J. Tetteh, J.S. Boateng, Development and characterisation of chitosan films impregnated with insulin loaded PEG-b-PLA nanoparticles (NPs): A potential approach for buccal delivery of macromolecules, *Int. J. Biol. Pharm. Allied Sci.* 428 (2012) 143–151.
- [9] N.E. Vrana, O. Erdemli, G. Francius, A. Fahs, M. Rabineau, C. Debry, A. Tezcaner, D. Keskin, P. Lavalle, Double entrapment of growth factors by nanoparticles loaded into polyelectrolyte multilayer films, *J. Mater. Chem. B* 2 (2014) 999–1008.
- [10] B.D. Ulery, L.S. Nair, T. Cato, C.T. Laurencin, Biomedical applications of biodegradable polymers, *J. Polym. Sci. B Polym. Phys.* 49 (2011) 832–864.
- [11] S.T. Yohe, Y.L. Colson, M.W. Grinstaff, Super hydrophobic materials for tunable drug release: using displacement of air to control delivery rates, *J. Am. Chem. Soc.* 134 (2012) 2016–2019.
- [12] <http://www.dailies.com>.
- [13] N.K. Al-Nemrawia, R.H. Dave, Formulation and characterization of acetaminophen nanoparticles in orally disintegrating films, *Drug Deliv.* 23 (2014) 540–549.
- [14] K.W. Ng, P.A. Torzilli, R.F. Warren, S. Maher, Characterization of a macroporous polyvinyl alcohol scaffold for the repair of focal articular cartilage defects, *J. Tissue Eng. Regen. Med.* 8 (2014) 164–168.
- [15] Whitney L. Stoppel, Joseph C. White, Sarena D. Horava, Surita R. Bhatia, Susan C. Roberts, Transport and stability of biological molecules in surfactant-alginate composite hydrogels, *Acta Biomater.* 7 (2011) 3988–3998.
- [16] M. Guzman, J. Molpeceres, F. Gracia, M.R. Aberturas, N. Rodriguez, Formation and characterization of cyclosporin loaded nanoparticles, *J. Pharm. Sci.* 82 (1993) 498–502.
- [17] M. Wulff-Pérez, A. Torcello-Gómez, M.J. Gálvez-Ruiz, A. Martín-Rodríguez, Stability of emulsions for parenteral feeding: preparation and characterization of o/w nanoemulsions with natural oils and pluronic F68 as surfactant, *Food Hydrocol.* 23 (2009) 1096–1102.
- [18] J. Grdadolnik, Y. Maréchal, Bovine serum albumin observed by infrared spectrometry. I. Methodology structural investigation, and water uptake, *Biopolymers* 62 (2001) 40–53.
- [19] Z. Li, X.W. Li, L.-Q. Zheng, X.-H. Lin, F. Geng, L. Yu, Bovine serum albumin loaded solid lipid nanoparticles prepared by double emulsion method, *Chem. Res. Chin. Univ.* 26 (2010) 136–141.
- [20] B.N. Bam, J.L. Cleland, J. Yang, M.Y. Manning, M.C. Manning, J.F. Carpenter, Tween protects recombinant human growth hormone against

- agitation-induced damage via hydrophobic interactions, *J. Pharm. Sci.* 87 (1998) 1554–1559.
- [21] C. Guo, J. Wang, X. Liang, L. Zheng, H. Liu, Effect of bovine serum albumin on the micellization of poly (ethylene oxide)-poly (propylene oxide)-poly (ethylene oxide) block copolymers in aqueous solutions by fluorescence spectroscopy, *Sci.China Chem. B* 49 (2006) 541–549.
- [22] B. Ojha, G. Das, Role of hydrophobic and polar interactions for BSA–amphiphile composites, *Chem. Phys. Lipids* 164 (2011) 144–150.
- [23] H. Gao, Y.N. Wang, Y.G. Fan, J.B. Ma, Synthesis of a biodegradable tadpole-shaped polymer via the coupling reaction of polylactide onto mono(6-(2-aminoethyl)amino-6-deoxy)- β -cyclodextrin and its properties as the new carrier of protein delivery system, *J. Control. Rel.* 107 (2005) 158–173.
- [24] A. Kondo, F. Murakami, K.O. Higashitani, Circular dichroism studies on conformational changes in protein molecules upon adsorption on ultrafine polystyrene particles, *Biotechnol. Bioeng.* 40 (1992) 889–894.